the plant journal

SEB Society for Experimental Biology

The Plant Journal (2018) **95,** 358–370 doi: 10.1111/tpj.13955

Metabolic reconstructions identify plant 3-methylglutaconyl-CoA hydratase that is crucial for branched-chain amino acid catabolism in mitochondria

Scott Latimer[1], Yubing Li[1], Thuong T.H. Nguyen[2,†], Eric Soubeyrand[1], Abdelhak Fatihi[3,‡], Christian G. Elowsky[3], Anna Block[4], Eran Pichersky[2] and Gilles J. Basset[1,*]

[1]*Department of Horticultural Sciences, University of Florida, Gainesville, Florida, 32611, USA,*

[2]*Department of Molecular, Cellular, and Developmental Biology, University of Michigan, Ann Arbor, Michigan, 48109, USA,*

[3]*Center for Plant Science Innovation, University of Nebraska-Lincoln, Lincoln, Nebraska, 68588, USA,*

[4]*Center for Medical, Agricultural and Veterinary Entomology, ARS, USDA, Gainesville, Florida, 32608, USA,*

[†] *Present address: Faculty of Biology and Biotechnology, Vietnam, National University – Ho Chi Minh City University of Science (VNU-HCMUS), Vietnam, Ho Chi Minh City, Vietnam, and*

[‡] *Present address: Institut Jean-Pierre Bourgin, UMR1318, INRA-AgroParisTech, Versailles, France*

Received 21 June 2016; revised 19 April 2018; accepted 24 April 2018; published online 9 May 2018.
*For correspondence (e-mail gbasset@ufl.edu).

SUMMARY

The proteinogenic branched-chain amino acids (BCAAs) leucine, isoleucine and valine are essential nutrients for mammals. In plants, BCAAs double as alternative energy sources when carbohydrates become limiting, the catabolism of BCAAs providing electrons to the respiratory chain and intermediates to the tricarboxylic acid cycle. Yet, the actual architecture of the degradation pathways of BCAAs is not well understood. In this study, gene network modeling in Arabidopsis and rice, and plant-prokaryote comparative genomics detected candidates for 3-methylglutaconyl-CoA hydratase (4.2.1.18), one of the missing plant enzymes of leucine catabolism. Alignments of these protein candidates sampled from various spermatophytes revealed non-homologous N-terminal extensions that are lacking in their bacterial counterparts, and green fluorescent protein-fusion experiments demonstrated that the Arabidopsis protein, product of gene *At4g16800*, is targeted to mitochondria. Recombinant At4g16800 catalyzed the dehydration of 3-hydroxymethylglutaryl-CoA into 3-methylglutaconyl-CoA, and displayed kinetic features similar to those of its prokaryotic homolog. When *at4g16800* knockout plants were subjected to dark-induced carbon starvation, their rosette leaves displayed accelerated senescence as compared with control plants, and this phenotype was paralleled by a marked increase in the accumulation of free and total leucine, isoleucine and valine. The seeds of the *at4g16800* mutant showed a similar accumulation of free BCAAs. These data suggest that 3-methylglutaconyl-CoA hydratase is not solely involved in the degradation of leucine, but is also a significant contributor to that of isoleucine and valine. Furthermore, evidence is shown that unlike the situation observed in Trypanosomatidae, leucine catabolism does not contribute to the formation of the terpenoid precursor mevalonate.

Keywords: branched-chain amino acid, catabolism, mitochondrion, senescence, ubiquinone, comparative genomics, *Arabidopsis thaliana*.

INTRODUCTION

Leucine, isoleucine and valine form the group of proteinogenic branched-chain amino acids (BCAAs), and are synthesized *de novo* solely by plants, fungi, archaea and bacteria. BCAAs are therefore essential to animals that acquire them from their diet and via symbiotic associations. While the biosynthesis of plant BCAAs and its associated regulatory mechanisms are for the most part well understood (Binder, 2010; Pratelli and Pilot, 2014; Xing and Last, 2017), our knowledge of the catabolism of these amino acids remains in comparison fragmentary (Hildebrandt *et al.*, 2015; Galili *et al.*, 2016). Yet, the catabolism of BCAAs is of particular significance, not only because it contributes to BCAA homeostasis, but also because it serves as an alternative energy source when carbohydrate

availability to plant tissues is restricted (Araújo *et al.*, 2011). This auxiliary supply of energy takes place at two levels: first, when electrons originating from the dehydrogenation of BCAA catabolic intermediates are fed into the respiratory chain; and second when their terminal catabolites enter the tricarboxylic acid cycle. Reflecting the crucial role of BCAAs as an alternative energy source for plant cells, *Arabidopsis thaliana* mutants corresponding to BCAA catabolic enzymes and their associated electron carrier proteins display accelerated senescence during dark-induced carbon starvation (Ishizaki *et al.*, 2005, 2006; Araújo *et al.*, 2010; Peng *et al.*, 2015). Recent evidence also indicates that this alternative pathway plays a role in drought tolerance (Pires *et al.*, 2016). The individual reactions of the BCAA degradation pathway in plants are similar to those of mammals and bacteria (Binder, 2010; Hildebrandt *et al.*, 2015). BCAAs are first deaminated into their cognate 2-oxo acids followed by their oxidative decarboxylation, and the resulting acyl-CoA thioesters are then oxidized and carboxylated to form enoyl-CoAs. Arabidopsis mutants have been identified for some of these steps, and their corresponding genes have been shown to encode mitochondrion-targeted enzymes (Gu *et al.*, 2010; Ding *et al.*, 2012; Angelovici *et al.*, 2013; Peng *et al.*, 2015). Downstream enzymes corresponding to β-hydroxyisobutiryl-CoA hydrolase, methylmalonate semialdehyde dehydrogenase and 3-hydroxyisobutyrate dehydrogenase in the degradation pathway of valine and to hydroxymethylglutaryl-CoA lyase in the degradation pathway of leucine have also been identified (Lange *et al.*, 2004; Lu *et al.*, 2011; Gipson *et al.*, 2017; Schertl *et al.*, 2017). By analogy with the degradation pathways of BCAAs in non-plant organisms, it is assumed that distinct hydratases catalyze the conversion of the enoyl-CoA catabolic intermediates (3-methyl-glutaconyl-CoA, methacrylyl-CoA and 2-methyl-but-2-enoyl-CoA for leucine, valine and isoleucine, respectively) into their cognate hydroxyl-acyl-CoAs (http://www.genome.jp/kegg-bin/show_pathway?map=map00280&show_description=show). The latter are then catabolized further into acetyl-CoA and succinyl-CoA (Galili *et al.*, 2016). Two Arabidopsis enoyl-CoA hydratase-like proteins have been proposed to correspond to the missing hydratases of BCAA catabolism based on their actual (At4g31810) or predicted (At3g60510) mitochondrial localization (Millar *et al.*, 2001; Binder, 2010). However, a hint that these proteins might not be the right candidates is that their corresponding genes do not co-express with those of other BCAA degradation enzymes (Binder, 2010). A later review of BCAA catabolic genes lists four additional enoyl-CoA hydratase candidates: At1g76150, At4g29010, At4g16800 and At4g16210 (Hildebrandt *et al.*, 2015). Adding to the confusion, there is evidence that plant peroxisomes contribute to the degradation of BCAA (Gerbling and Gerhardt, 1989; Lange *et al.*, 2004), and proteomics and green fluorescent protein (GFP)-fusion studies in Arabidopsis have identified enoyl-CoA hydratases that are targeted to peroxisomes (Reumann *et al.*, 2007; Eubel *et al.*, 2008).

In this study, as part of a systems biology effort aimed at reconstructing the functional networks of genes that are functionally linked to electron transport chains in plant organelles, we identified orthologous 3-methylglutaconyl-CoA hydratase candidates as node connectors between respiration and BCAA degradation. We investigated the subcellular localization and *in vitro* activity of the Arabidopsis enzyme, and examined the physiological and biochemical impact of knocking out its cognate gene.

RESULTS

Plant-prokaryote comparative genomics points to crotonase-like homologs that are functionally linked to respiration and leucine catabolism

Co-expression analyses of the *A. thaliana* probe sets of the ATTED-II (Aoki *et al.*, 2016) and GeneCAT (Mutwil *et al.*, 2008) microarray databases detected *At4g16800* as a remarkable functional node between genes involved in mitochondrial respiration (Figure 1a). These include subunits of mitochondrial ATP synthase and cytochrome C oxidase, components of Complex I of the respiratory chain, and enzymes required for the biosynthesis of ubiquinone (coenzyme Q), an essential electron carrier of the mitochondrial inner membrane (Figure 1a; Dataset S1). *At4g16800* is predicted to encode for a 31-kDa protein of unknown cellular function. It displays, however, a conserved crotonase-like domain (cd065580) commonly found in enzymes acting on acyl-CoA intermediates (Holden *et al.*, 2001). Searching the SEED database for comparative genomics (Overbeek *et al.*, 2005) with the protein sequence of At4g16800 as query identified bacterial homologs in Firmicutes, Proteobacteria and Actinobacteria, whose corresponding genes are organized in canonical operons (Figure 1b). Coinciding with such an arrangement, six of the seven genes that make up these clusters map onto consecutive reactions of the reference pathway for leucine degradation in the KEGG database (Figure 1c). Among these, the prokaryotic homologs of *At4g16800* match with 3-methylglutaconyl-CoA hydratase (4.2.1.18) that catalyzes the reversible conversion of 3-methylglutaconyl-CoA into 3-hydroxy-3-methylglutaryl-CoA (Figure 1c). Inspection of the co-expression profile of *At4g16800* in microarray and RNA sequencing experiments confirmed that in Arabidopsis as well the expression of this gene is co-regulated with that of genes involved in the catabolism of BCAA (Figure 1d; Dataset S1). Similar results were obtained for *Os02g0654100*, the rice ortholog of *At4g16800* (Figure 1d; Dataset S1). Moreover, as is classically observed for BCAA catabolic genes, *At4g16800* is expressed in all plant organs (Figure S1). This cross-examination of plant

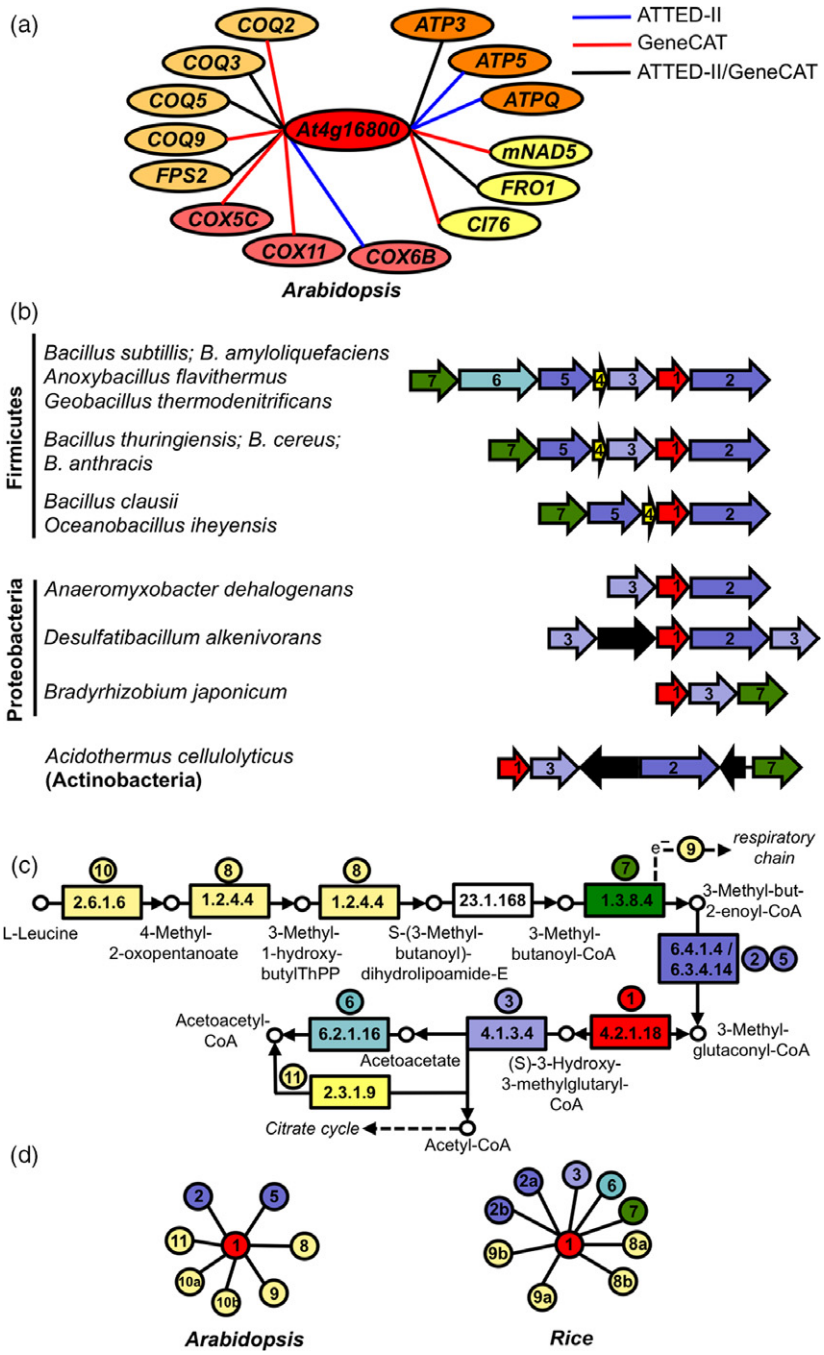

Figure 1. Functional network of *At4g16800* and metabolic reconstructions.
(a) Arabidopsis genes encoding for ubiquinone biosynthetic enzymes COQ2, COQ3, COQ5, COQ9 and FPS2, cytochrome C oxidase subunits COX5C, COX11 and COX6B, NADH-ubiquinone oxidoreductase subunits CI76, FRO1 and mNAD5, and ATP synthase subunits ATPQ, ATP5 and ATP3 were used as baits to mine the ATTED-II and Gene-CAT microarray databases. Blue, red and black lines denote co-expression detected in ATTED-II, GeneCAT or both databases, respectively. The gene lists resulting from these searches are provided as Dataset S1.
(b) Comparative genomics of *At4g16800*. Prokaryotic homologs of *At4g16800* and their genomic context were mined from the SEED database. Matching color and number indicate homology. Black arrows indicate genes of unknown function or of function *a priori* unrelated to leucine degradation.
(c) Overlay of functional assignments from SEED on KEGG reference map 00280.
(d) Interaction networks reconstituted from the 2000 top co-expressors of *At4g16800* and top 300 co-expressors of rice ortholog (*Os02g0654100*). The annotated gene lists resulting from these searches are provided as Dataset S1. 1, 3-methylglutaconyl-CoA hydratase (4.2.1.18); 2, methylcrotonyl-CoA carboxylase (6.4.1.4); 3, hydroxymethylglutaryl-CoA lyase (4.1.3.4); 4, biotin carboxyl carrier protein of methylcrotonyl-CoA carboxylase; 5, biotin carboxylase of methylcrotonyl-CoA carboxylase (6.3.4.14); 6, acetyl-CoA synthetase (6.2.1.16); 7, isovaleryl-CoA dehydrogenase (1.3.8.4); 8, 3-methyl-2-oxobutanoate dehydrogenase (1.2.4.4); 9, electron transfer flavoprotein; 10, branched-chain amino acid (BCAA) transferase (2.6.1.42); 11, acetyl-CoA C-acetyltransferase (2.3.1.9).

transcriptomics databases and prokaryotic genomes thus not only indicates that there are some conserved functional associations between At4g16800, mitochondrial respiration and leucine catabolism, but also designates At4g16800 and its plant orthologs as strong candidates for the missing 3-methylglutaconyl-CoA hydratase of leucine catabolism in plants.

At4g16800 is localized in mitochondria

Alignments of At4g16800 and its orthologs sampled from various spermatophytes revealed non-homologous N-terminal regions of 25–60 residues that are absent in their bacterial homolog (Figure 2a). Analyses performed with TargetP (Emanuelsson *et al.*, 2000), iPSORT (Bannai *et al.*, 2002) and Predotar (Small *et al.*, 2004) resulted in the prediction of targeting of At4g16800 to the mitochondrion, while seven of At4g16800's top 14 nearest neighbors predicted by Wolf Psort (Horton *et al.*, 2007) were mitochondrial (Table S1). When an expression construct corresponding to the fusion of GFP to the C-terminal end of At4g16800 was co-infiltrated in *Nicotiana benthamiana* epidermal cells with that of a red fluorescent protein (RFP)-tagged isovaleryl-CoA dehydrogenase mitochondrial marker, confocal laser-scanning microscopy experiments confirmed that the fluorescent reporter proteins strictly co-localized (Figure 2b–d). Time-lapse acquisitions further verified that the small punctate structures associated with the green and red fluorescence overlay moved rapidly within cytosolic streams around the nucleus and the vacuole as is typically observed for mitochondria (Video S1).

In vitro activity of At4g16800

A 6x-histidine-tagged version of the At4g16800 protein lacking its predicted N-terminal pre-sequence (residues 1–42) was expressed in *Escherichia coli*. The dehydratase activity of the purified enzyme was then assayed with 3-hydroxymethylglutaryl-CoA as the substrate, quantifying the formation of 3-methylglutaconyl-CoA by reverse-phase high-performance liquid chromatography (HPLC) coupled to spectrophotometric detection. These assays resulted in typical Michaelian kinetics with K_m, V_{max}, K_{cat} and K_{cat}/K_m values of 53.1 ± 7.7 μM, 774.2 ± 43.2 nmol sec^{-1} mg^{-1},

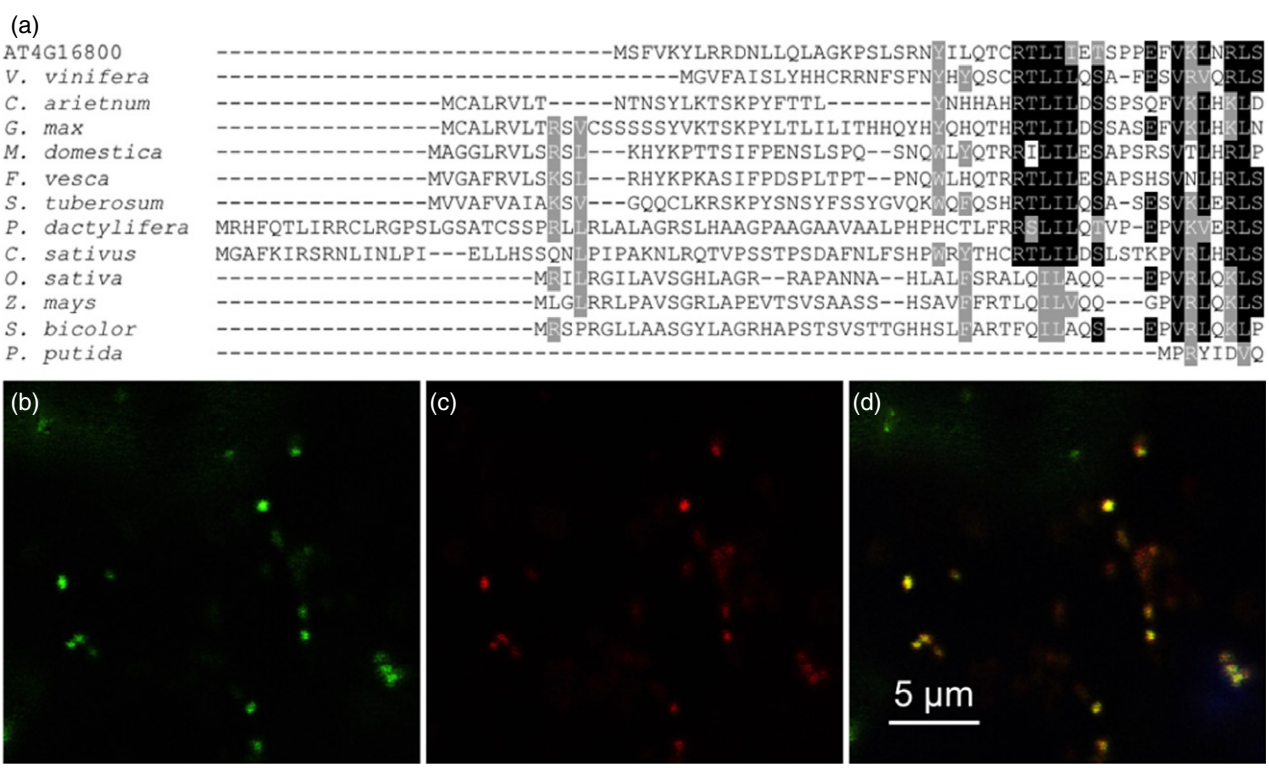

Figure 2. Subcellular localization of At4g16800.
(a) Alignment of the N-terminal regions of At4g16800 and its orthologs in grape vine (*Vitis vinifera*), chickpea (*Cicer arietinum*), soybean (*Glycine max*), apple (*Malus domestica*), strawberry (*Fragaria vesca*), potato (*Solanum tuberosum*), date palm (*Phoenix dactylifera*), cucumber (*Cucumis sativus*), rice (*Oryza sativa*), maize (*Zea mays*), sorghum (*Sorghum bicolor*) and the γ-proteobacterium *Pseudomonas putida*. Identical and similar residues are shaded in black and gray, respectively. Dashes represent gaps introduced to maximize alignment.
(b) Confocal laser-scanning microscopy imaging of At4g16800 (minus its stop codon) fused to the N-terminus of green fluorescent protein (GFP) and transiently expressed in *Nicotiana benthamiana* epidermal cells.
(c) Red pseudocolor of mitochondrial marker red fluorescent protein (RFP)-tagged isovaleryl-CoA dehydrogenase co-infiltrated with At4g16800-GFP.
(d) Overlay of green and red pseudocolors.

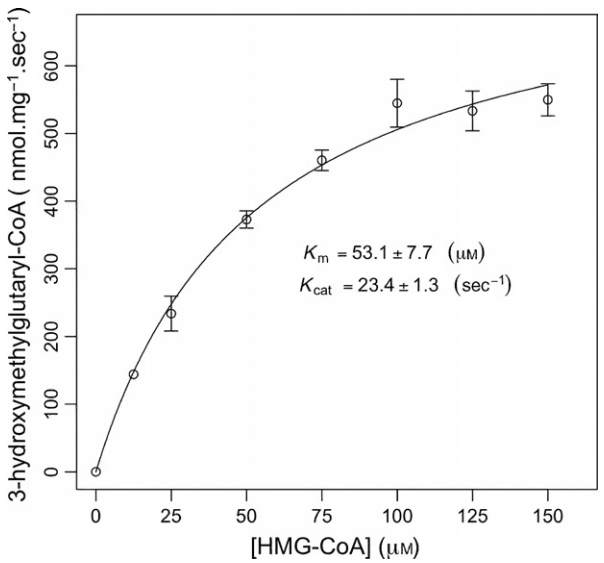

Figure 3. *In vitro* assays and kinetic properties of recombinant At4g16800. Assays contained 0.125 μg of recombinant At4g16800 and 3-hydroxymethylglutaryl-CoA (3-HMG-CoA) at the indicated concentrations, and were carried out for 5–20 min at 30°C. Data are means of three replicates ± SE.

23.4 ± 1.3 sec^{-1} and 0.44 μM^{-1} sec^{-1}, respectively (Figure 3). These kinetic parameters are similar to those reported for 3-methylglutaconyl-CoA hydratase purified from Acinetobacter sp. cells and assayed in similar conditions (36 μM, 60 sec^{-1} and 1.7 μM^{-1} sec^{-1} for K_m, K_{cat} and K_{cat}/K_m, respectively; Mack *et al.*, 2006a).

At4g16800 knockout plants display accelerated senescence in response to extended darkness conditions

To directly investigate the *in vivo* function of *At4g16800*, indexed collections of Arabidopsis mutants were searched using the T-DNA Express gene-mapping tool of the SALK Institute (http://signal.salk.edu/cgi-bin/tdnaexpress). Four T-DNA lines corresponding to insertions in the 5′-untranslated region (SAIL_428_H01), third intron (GABI_008D11) and 3′-untranslated region (SALK_072957, SALK_026612C) of *At4g16800* were identified and confirmed by DNA genotyping (Figure S2). Reverse transcriptase-polymerase chain reaction (RT-PCR) analyses using a primer pair designed to amplify a cDNA region spanning from the third exon to the seventh exon of *At4g16800* showed that only the T-DNA insertion corresponding to line GABI_008D11 resulted in the absence of detectable transcripts (Figure S2). Complemented transgenics (30-7) were therefore generated as a control via transformation of the GABI_008D11 mutant with *At4g16800*'s full-length cDNA under the control of the 35S promoter (Figure S2).

When grown in 12-h days, wild-type, GABI_008D11 and complemented 30-7 (GABI_008D11-35S::*At4g16800* cDNA) plants were visually indistinguishable (Figure 4a). Similarly, no statistically significant differences in silique length, number of seeds per silique, seed weight and germination rate were observed between wild-type and GABI_008D11 plants (Table S2). However, when plants were transferred into darkness for 10 days, conditions that are known to promote protein and amino acid catabolism (Ishizaki *et al.*, 2005, 2006; Engqvist *et al.*, 2010; Peng *et al.*, 2015), and then allowed to recover for 15, 30 and 45 days in 12-h days, the GABI_008D11 mutant did not recover (Figure 4a). Such a phenotype resembles the accelerated senescence response to extended darkness conditions that has been described for mutants of leucine and other BCAA catabolism in plants (Ishizaki *et al.*, 2005, 2006; Peng *et al.*, 2015). Also notable is that the GABI_008D11 mutant did not display the defects in seed development and germination that have been reported for Arabidopsis mutants corresponding to 3-methylcrotonyl-CoA carboxylase (6.4.1.4/6.3.4.14; Figure 1; Ding *et al.*, 2012).

3-Methylglutaconyl-CoA hydratase activities were readily detected in green (0 day) and senescent rosette leaves (5 and 10 days of dark treatment), as well as seeds of wild-type and complemented plants (Figure 4b). As expected, 35S-driven overexpression of *At4g16800*'s cDNA in the complemented mutant resulted in the highest specific activities both in leaves and seeds (Figure 4b). By contrast, either no activity (green and 5 day dark-treated leaves and seeds) or only background activity (10 day dark-treated leaves) were detected in the GABI_008D11 knockout (Figure 4b). These data indicate that At4g16800 is the major, when not sole, enoyl-CoA hydratase displaying 3-methylglutaconyl-CoA hydratase activity in leaves and seeds.

At4g16800 knockout plants display marked defects in the catabolism of BCAA

Consistent with the absence of visible differences in phenotype between wild-type, GABI_008D11 and complemented mutant plants under standard light regime, the rosette leaves of these plants did not display any statistically significant differences in the levels of free proteinogenic amino acids when grown in 12-h days (Figure 5). By contrast, subjecting the plants to 2, 5 and 10 days of dark treatment revealed striking differences in the kinetics of accumulation of several free amino acids (Figure 5). Most notably, between 2 and 5 days of dark treatment leucine, isoleucine and valine accumulated approximately 1.2–5.6 times faster in the GABI_008D11 mutant than in the wild-type and the complemented mutant (Figure 5). After 10 days, the content of leucine, isoleucine and valine measured in the leaves of the GABI_008D11 mutant reached approximately 22-, 6- and 2.5-fold that of the controls, respectively (Figure 5). In fact, added together these three BCAAs represented after 10 days of dark treatment about 50% of total free amino acids in the knockout as compared with 26% and 16% for the wild-type and complemented mutant controls, respectively. Meanwhile, methionine level was 2.3-fold higher in

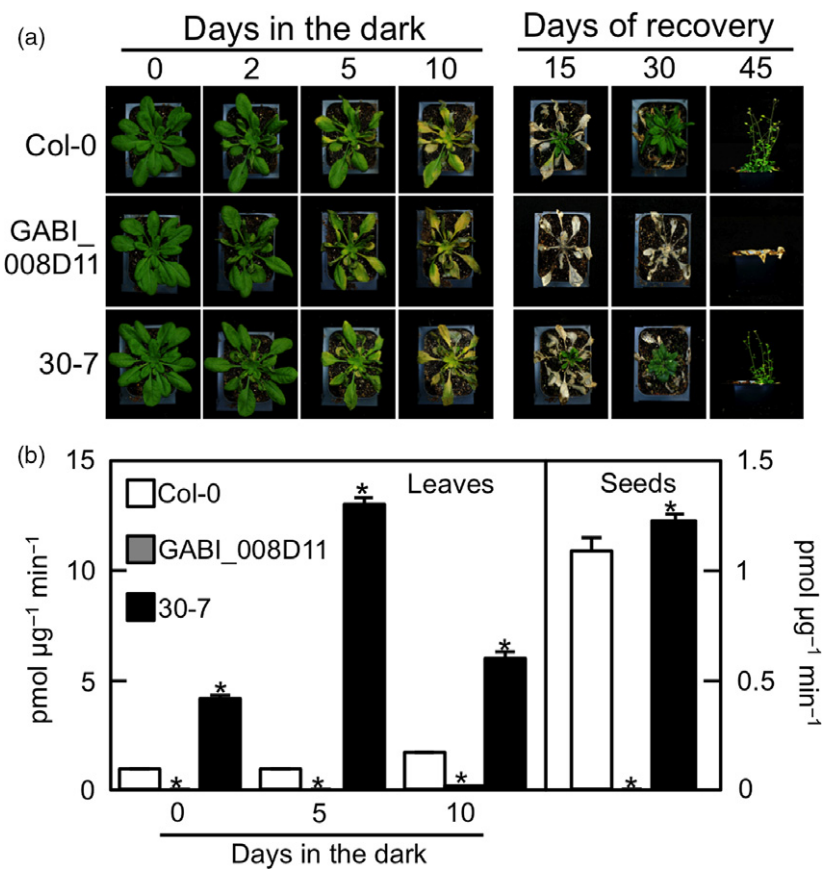

Figure 4. Phenotypic characterization and 3-methylglutaconyl-CoA hydratase assays in leaves and seed extracts.
(a) Phenotypes of 4 week-old wild-type (Col-0), GABI_008D11 and complemented 30-7 plants grown in 12-h days (0), transferred into darkness for 2, 5 or 10 days, and then allowed to recover for 15, 30 and 45 days in 12-h days (110 µE m^{-2} sec^{-1}).
(b) 3-Methylglutaconyl-CoA hydratase activity in rosette leaves and seed extracts of 4-week-old wild-type (Col-0), GABI_008D11 and complemented 30-7 plants. Green leaves (0) and senescent leaves (5, 10) were harvested on plants grown in 12-h days and plants transferred into darkness for 5 or 10 days, respectively. Data are means of three replicates at a substrate concentration of 150 µM ± SD. Asterisks indicate statistically significant differences with wild-type plants as determined by Fisher's test ($P < \alpha = 0.05$) from an analysis of variance.

the GABI_008D11 mutant than in the controls (Figure 5). All together, these changes resulted after 10 days of dark treatment in a twofold increase in the total content of free amino acids in the leaves of the knockout as compared with those of the controls (Figure 5). In contrast, dark-treated SAIL_428_H01, SALK_072957 and SALK_026612C plants that were homozygous for their cognate T-DNA insertion did not display any statistically significant increase in BCAA levels comparatively to the control (Figure S3), thus confirming that these T-DNA lines are not knockouts. These lines were therefore not investigated further.

The large increase in BCAA levels in the leaves of dark-treated knockout plants was still visible after acidic hydrolysis of leaf protein extracts; the total level of leucine, isoleucine and valine for the GABI_008D11 plants being 2.2-, 1.6- and 1.3-fold higher than that of the controls, respectively (Figure 6). That there was no statistically significant difference in leaf protein contents between knockout and controls plants showed that such an increase in total BCAAs in the GABI_008D11 line was exclusively due to an increase in the free pools of these amino acids; the contribution of free leucine, isoleucine and valine to their respective total pool being 38%, 34% and 41% in the knockout as compared with 5%, 10% and about 20% in the controls (Figures 5 and 6). The profile of free amino acid of seeds harvested from homozygous knockout, wild-type and complemented plants recapitulated the prominent difference in BCAA content observed in senescing leaves, with leucine, isoleucine and valine accumulating approximately 88-, 34- and 13-fold their level in the controls, respectively (Figure 7a). The contribution of BCAAs to total free amino acids was approximately 10 times higher in the seeds of the GABI_008D11 mutant (49%) than in those of the wild-type (4%) and the complemented mutant (5%). Besides BCAAs, aspartate, serine and histidine also displayed consistently higher levels in the GABI_008D11 seeds as compared with the controls; the increase ranging from two- to threefold for aspartate and serine to 11-fold for histidine (Figure 7a). Similar to the situation observed in senescing leaves, the total content of free proteinogenic amino acids in the GABI_008D11 seeds was 1.6- to 3.5-fold higher than that of the controls (Figure 7a). Such differences, however, were no longer noticeable after acidic hydrolysis (Figure 7b).

DISCUSSION

We provide here comparative genomics, biochemical and genetic evidence that Arabidopsis gene *At4g16800* encodes the missing 3-methylglutaconyl-CoA hydratase (4.2.1.18) of the leucine degradation pathway. This enzyme and its

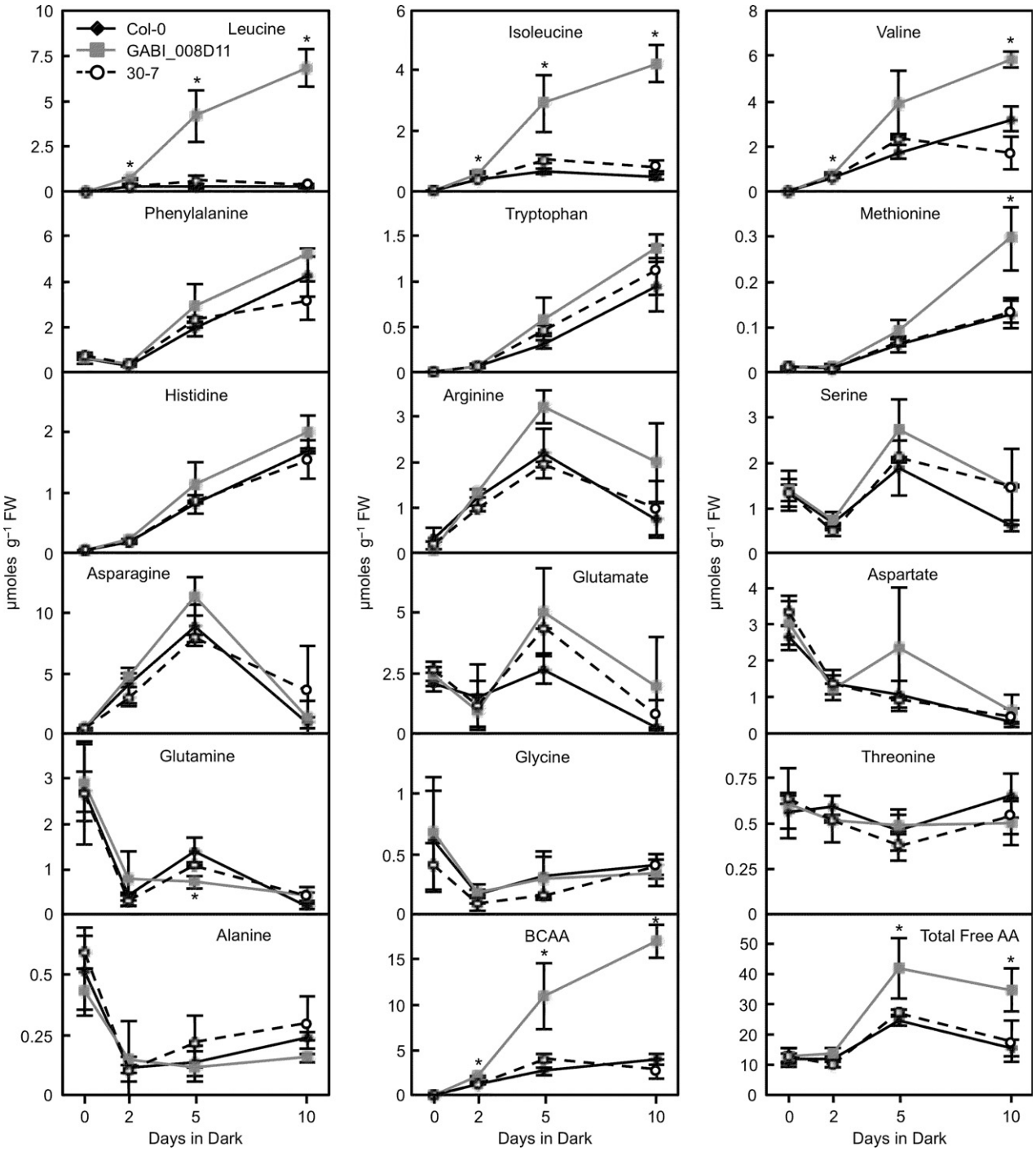

Figure 5. Levels of free proteinogenic amino acids in Arabidopsis leaves.
Rosette leaves were collected on 4-week-old wild-type (Col-0), GABI_008D11 and complemented 30-7 plants grown in 12-h days (0), and after these plants were transferred into darkness for 2, 5 or 10 days. Values are the means of three experimental replicates ± SD. Asterisks indicate statistically significant differences between GABI_008D11 and control (Col-0 and complemented 30-7) plants as determined by Fisher's test ($P < \alpha = 0.05$) from an analysis of variance. BCAA, branched-chain amino acid.

corresponding gene were previously known in only a few organisms (Rodríguez *et al.*, 2004; Wong and Gerlt, 2004; Mack *et al.*, 2006a,b); most of the literature focusing on the human ortholog, the loss of function of which results in metabolic and neurological disorders (Di Rosa *et al.*, 2006). Our data indicate that Arabidopsis 3-methylglutaconyl-CoA hydratase is targeted to the mitochondrion, which is consistent with the localization of the mammalian enzyme

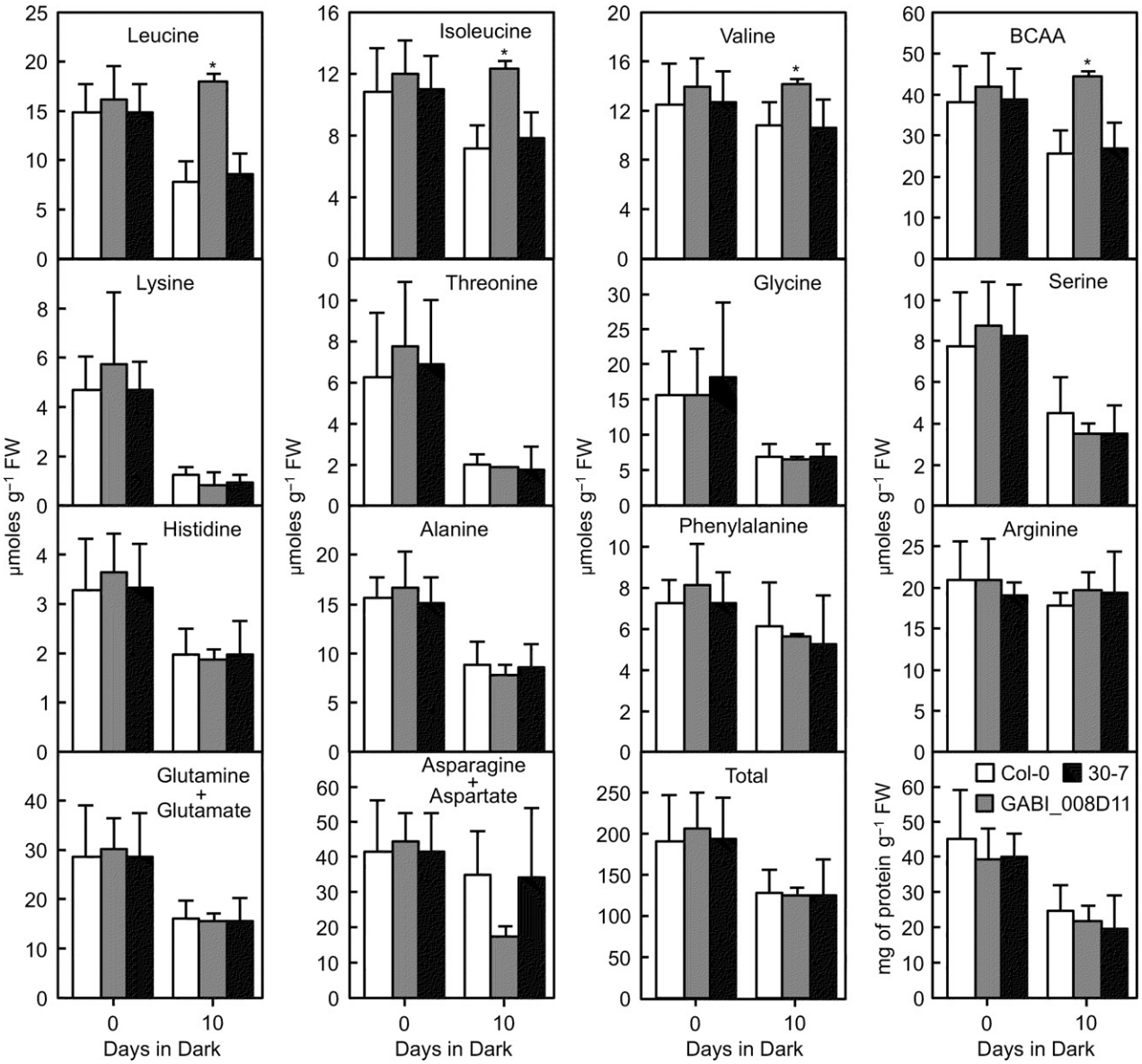

Figure 6. Levels of total proteinogenic amino acids in Arabidopsis leaves.
Rosette leaves were collected on 4-week-old wild-type (Col-0, white bars), GABI_008D11 (gray bars) and complemented 30-7 (black bars) plants grown in 12-h days (0), and after these plants were transferred to darkness for 10 days. Values are the means of three-four experimental replicates ± SD. Asterisks indicate statistically significant differences between GABI_008D11 and control (Col-0 and complemented 30-7) plants as determined by Fisher's test ($P < \alpha = 0.05$) from an analysis of variance. BCAA, branched-chain amino acid.

(Mack *et al.*, 2006b). Plant mitochondria thus possess the full-set of enzymes required for the degradation of leucine at least up to the formation of acetoacetate by hydroxymethylglutaryl-CoA lyase (Taylor *et al.*, 2004).

Gene network reconstructions point to the existence of prominent functional associations between *At4g16800* and some components of the respiratory chain, including most strikingly five enzymes involved in the biosynthesis of the redox co-factor ubiquinone (Figure 1a). Because in plants the prenyl side-chain of ubiquinone originates from mevalonate (Disch *et al.*, 1998), the immediate precursor of which is 3-hydroxy-3-methylglutaryl-CoA, our data invite the question of whether the mitochondrial pool of this metabolite produced by 3-methylglutaconyl-CoA hydratase could contribute to the biosynthesis of ubiquinone. This scenario seems *a priori* plausible, especially in conditions of increased BCAA catabolism, for there exists a similar precedent in Trypanosomatidae, which are able to derive their prenyl precursors from the intact skeleton of leucine (Ginger *et al.*, 2001). The International Union of Biochemistry and Molecular Biology has actually classified 3-methylglutaconyl-CoA hydratase as a mevalonate

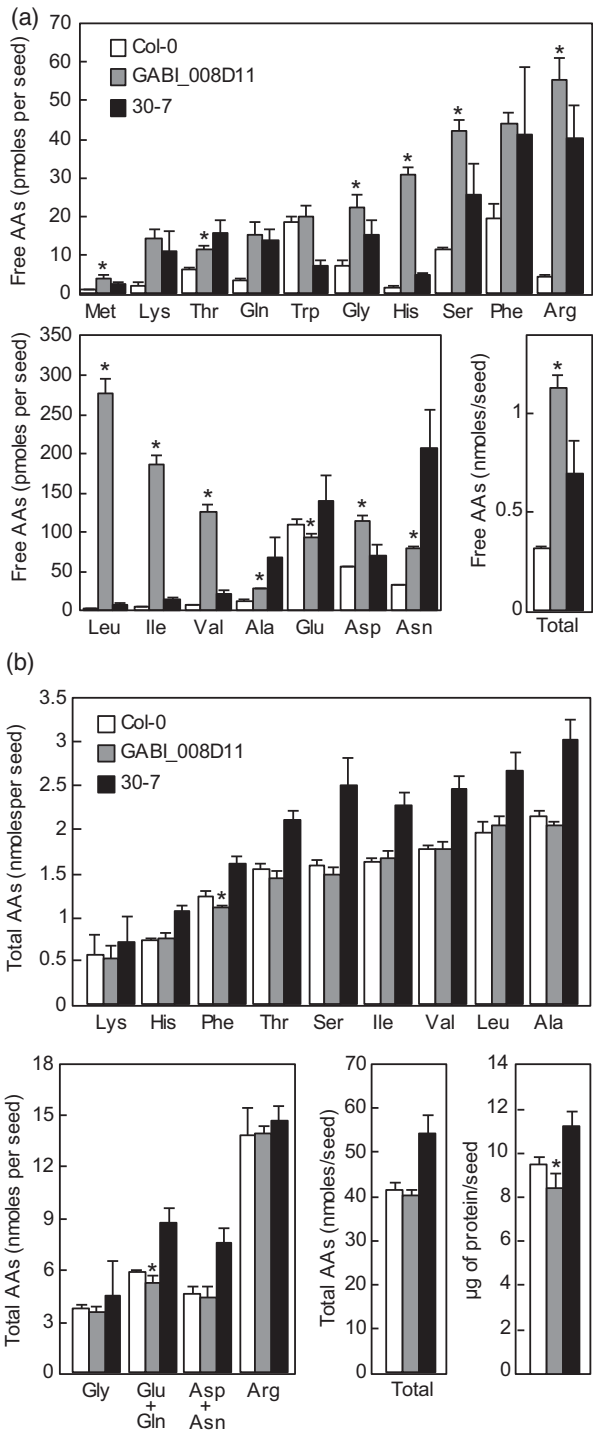

Figure 7. Levels of free and total proteinogenic amino acids (AAs) and protein content in Arabidopsis seeds.
(a) Free proteinogenic amino acids.
(b) Total proteinogenic amino acids and protein content. Values are the means of four experimental replicates ± SD. Asterisks indicate statistically significant differences between GABI_008D11 and control (Col-0 and complemented 30-7) plants as determined by Fisher's test ($P < \alpha = 0.05$) from an analysis of variance.

biosynthetic enzyme (http://www.chem.qmul.ac.uk/iubmb/enzyme/reaction/terp/MVA.html). However, quantification of ubiquinone in Arabidopsis seeds and leaves showed no statistically significant differences between the *at4g16800* knockout and wild-type control plants (Figure S4). These results indicate that in Arabidopsis 3-methylglutaconyl-CoA hydratase does not contribute to ubiquinone biosynthesis, and verify the standard model in which plant mevalonate is synthesized exclusively in the cytosol (Vranová *et al.*, 2013). With such a hindsight, it appears that *At4g16800* owes its occurrence in the functional network of ubiquinone biosynthetic genes to the fact that electrons originating from the dehydrogenation of isovaleryl-CoA (1.3.8.4; Figure 1c), two steps upstream of that catalyzed by 3-methylglutaconyl-CoA hydratase, are transferred to ubiquinone in the inner membrane of mitochondria via the electron transfer flavoprotein and electron transfer flavoprotein: ubiquinone oxidoreductase (Ishizaki *et al.*, 2005, 2006; Araújo *et al.*, 2010). Furthermore, the electron transfer flavoprotein/electron transfer flavoprotein: ubiquinone oxidoreductase system, which is transcriptionally activated during dark-induced senescence, is also known to feed to the mitochondrial respiratory chain electrons generated during phytol and lysine degradation (Buchanan-Wollaston *et al.*, 2005; Ishizaki *et al.*, 2005, 2006; Araújo *et al.*, 2010).

Knocking out Arabidopsis, 3-methylglutaconyl-CoA hydratase results not only in the accumulation of leucine, but also in that of isoleucine and valine. Similar concurrent increases in the levels of all three BCAAs have also been observed in Arabidopsis mutants corresponding to enzymes located upstream and downstream of 3-methylglutaconyl-CoA hydratase, i.e. BCAA transferase 2 (At1g10070; Angelovici *et al.*, 2013; Peng *et al.*, 2015), subunits of the branched-chain keto dehydrogenase complex (At1g21400, At5g09300, At3g13450; Peng *et al.*, 2015), isovaleryl-CoA dehydrogenase (At3g45300; Gu *et al.*, 2010; Peng *et al.*, 2015), subunits A and B of methylcrotonyl-CoA carboxylase (At1g03090, At4g34030; Ding *et al.*, 2012), and hydroxymethyl-glutaryl-CoA lyase (At2g26800; Peng *et al.*, 2015). Moreover, two enzymes of the valine degradation pathway, 3-hydroxyisobutyrate dehydrogenase (At4g20930) and methylmalonate semialdehyde dehydrogenase (At2g14170), were recently shown to contribute to isoleucine and leucine catabolism, respectively (Gipson *et al.*, 2017; Schertl *et al.*, 2017). Our data thus agree with the consensual view that driven by the structural similarities of proteinogenic BCAAs and their catabolic intermediates, plants have evolved the capacity to degrade these metabolites via some shared enzymes (Binder, 2010; Hildebrandt *et al.*, 2015). Such an architecture contrasts starkly with that of mammals, which possess a fully separate pathway to catabolize valine (Shimomura *et al.*, 1994). Of particular

interest in this dedicated metabolic route is the presence of an enoyl-CoA hydratase (4.2.1.17), called methacrylyl-CoA hydratase, whose catalytic mechanism is closely related to that of 3-methylglutaconyl-CoA hydratase (4.2.1.18). Methacrylyl-CoA hydratase is thought to be critical to mammalian cells as it converts methacrylyl-CoA, a thiol-reactive and highly cytotoxic metabolite, into 3-hydroxyisobutyryl-CoA, which is then irreversibly deacylated into non-toxic 3-hydroxyisobutyrate (Brown *et al.*, 1982; Shimomura *et al.*, 1994; Ishigure *et al.*, 2001). As compounding evidence points to the existence of shared enzymes in the catabolism of all three proteinogenic BCAAs in plants, it is tempting to speculate that plant 3-methylglutaconyl-CoA hydratase moonlights on methacrylyl-CoA and prevents its accumulation. If so, the dual nature of plant 3-methylglutaconyl-CoA hydratase as contributor to the generation of an auxiliary supply of energy and detoxifying enzyme might explain in part why its cognate knockout does not recover from extended darkness conditions. It should be mentioned, however, that this increased sensitivity to prolonged darkness and its associated phenotype of accelerated leaf senescence are shared here again with other mutants of BCAA catabolism (Ishizaki *et al.*, 2005, 2006; Araújo *et al.*, 2010; Peng *et al.*, 2015). Furthermore, mutants impaired in the catabolism of glutamate and lysine, which also contribute to energy production during carbon-limiting conditions, also display increased susceptibility to dark treatments (Miyashita and Good, 2008; Araújo *et al.*, 2010). The large increase in BCAA levels was also observed in dry seeds of the 3-methylglutaconyl-CoA hydratase knockout. Such metabolic changes, which we attribute to the senescence-like process occurring in the seed coat during desiccation, are congruent with the proposal that BCAA catabolism in the tissues of the ovule may contribute to the energy status of developing seeds (Galili *et al.*, 2014). Our data show, however, that at least in controlled laboratory conditions the presence of 3-methylglutaconyl-CoA hydratase in maternal tissues is not vital for seed development. Lastly, the finding that the loss of function of 3-methylglutaconyl-CoA hydratase boosts total BCAAs levels specifically in senescing tissues and without adverse effects on seed germination and development, opens a new avenue for breeding and biotechnological strategies aimed at improving the nutritional quality of plant-based food. This is particularly relevant for leucine, the supplementation of which to the diet of farm animals is known to increase muscle and milk protein synthesis (Dunshea *et al.*, 2005; Murgas Torrazza *et al.*, 2010; Zhang *et al.*, 2016).

EXPERIMENTAL PROCEDURES

Bioinformatics

The ATTED-II (Aoki *et al.*, 2016) and GeneCAT (Mutwil *et al.*, 2008) co-expression databases were mined using Arabidopsis respiratory genes *At4g19010*, *COQ2* (*At4g23660*), *COQ3* (*At2g30920*), *COQ5* (*At5g57300*), *COQ9* (*At1g19140*), *SPS3* (*At2g34630*), *FPS2* (*At4g17190*), *ABC1* (*At4g01660*), *COX5C* (*At5g61310*), *COX10* (*At2g44520*), *COX11* (*At1g02410*), *COX15* (*At5g56090*), *COX17* (*At3g15352*), *COX6B* (*At1g22450*), *CB5-A* (*At1g26340*), *CI76* (*At5g37510*), *FRO1* (*At5g67590*), *MFDX2* (*At4g21090*), *SURF1* (*At3g17910*), *OXA1* (*At5g62050*), *HCC1* (*At3g08950*), *ATPQ* (*At3g52300*), *ATP3* (*At2g33040*), *ATP5* (*At5g13450*), *mNAD5* (*Atmg00513*), *mNAD7* (*Atmg00510*). The top 1500 co-expressors of each of these genes were then aggregated using jvenn (http://jvenn.toulouse.inra.fr/app/example.html). Genes that intersected with six or more of the query respiratory genes were selected, resulting in a list of 289 co-expressors. Genes of unknown cellular function were isolated from this subset of co-expressors and individually subjected to comparative genomics and co-expression analyses. Prokaryotic homologs of *At4g16800* and their respective genomic neighborhood (8 kb upstream and downstream, totaling 16 kb) were retrieved from the SEED database for comparative genomics (http://pubseed.theseed.org) using At4g16800 as a query in BLASTp search mode. Enzymatic functions identified in SEED were overlaid on the leucine degradation pathway using KEGG map 00280 (http://www.genome.jp/kegg/pathway.html). The functional interactions of *At4g16800* and of its rice ortholog (*Os02g0654100*) with BCAA catabolic genes were mined from the top 2000 and top 300 co-expressors of each of these two genes in ATTED-II, respectively.

Plant material and growth conditions

T-DNA insertion mutants SAIL_428_H01, GABI_008D11, SALK_072957 and SALK_026612C were obtained from the Arabidopsis Biological Resource Center at the Ohio State University (Alonso *et al.*, 2003). Plants were grown on potting mix in a growth chamber at 22°C in 12-h days (100–110 μE m^{-2} sec^{-1}) for 4–5 weeks. Dark treatments were conducted on 4–5-week-old plants for 10 days. For recovery experiments, dark-treated plants were transferred back to 12-h days (110 μE m^{-2} sec^{-1}) light regime for 15, 30, 45 days. For germination assays, seeds were placed on Murashige and Skoog solid medium containing sucrose (10 g L^{-1}), stratified for 5 days at 4°C, and then transferred at 22°C in 12-h days (110 μE m^{-2} sec^{-1}). Germination was scored after 5 days based on the emergence of cotyledons.

Plant genotyping and RT-PCR analyses

Arabidopsis mutants originated from the SAIL (Sessions *et al.*, 2002), GABI-Kat (Kleinboelting *et al.*, 2012) and SALK (Alonso *et al.*, 2003) collections. Plants were genotyped using the following combination of primers: LP1 5′-AGCATCGGTTTGTTCAAACAC-3′, RP1 5′-AAGCTGGGGAGGATAACACAG-3′ and T-DNA-specific LB1 5′-GCCTTTTCAGAAATGGATAAATAGCCTTGCTTCC-3′ for SAIL_428_H01; LP2 5′-TTCCTTTGATACCGATCTCCC-3′, RP2 5′-ACAAACC GATGCTAAGGGAAC-3′ and T-DNA-specific o8760 5′-GGGC TACACTGAATTGGTAGCTC-3′ for GABI_008D11; LP3 5′-AGACGTT CGAGATAATTGCCC-3′, RP3 5′-TTGGCAATGTACCCAAAGAAG-3′ and T-DNA-specific LBb1 5′-GCGTGGACCGCTTGCTGCAACT-3′ for SALK_072957 and SALK_026612C. RT-PCR analyses were performed on total RNA extracted from Arabidopsis leaves using the RNAeasy Plant Mini Kit (Qiagen, Germantown, MD, USA). PCR was performed on cDNAs prepared from 1 μg of total RNA using the following gene-specific primers: RTfwd, 5′-AGAACTATGAGTC-CATCTGA-3′ (forward) and RTrvs 5′-TATTAAGAAGCTTCTGA-TAACA-3′ (reverse) for *At4g16800*; and 5′-CTAAGCTCTCAA-GATCAAAGGC-3′ (forward) and 5′-TTAACATTGCAAAGAGTTT-CAAGG-3′ (reverse) for the actin control.

Complementation of the At4g16800 knockout

Full-length *At4g16800* cDNA was sub-cloned into plant expression vector pB2GW7 (Karimi *et al.*, 2002) under the control of the 35S promoter using Gateway technology. The resulting construct was then introduced into the GABI_008D11 line using the floral dip method (Clough and Bent, 1998), and transformants (T1) were selected on soil by applications of glufosinate (120 mg L^{-1}) every other day. Detached and dark-treated leaves of T2 lines were screened by HPLC-fluorescence analysis to identify plants having wild-type level of leucine. Homozygous complemented lines were isolated by examining the germination ratio of the T3 progeny on plates containing glufosinate (20 mg L^{-1}).

Subcellular localization

At4g16800 cDNA was amplified minus its stop codon using primers 5′-CACCATGAGCTTCGTCAAGTATCTCCG-3′ (forward) and 5′-ATTGCCAGTGTACAGAGGCTTA-3′ (reverse). This PCR product was cloned into pENTR/D-TOPO (Invitrogen, Waltham, MA, USA) and then transferred into pK7FWG2 (Karimi *et al.*, 2002) using Gateway technology (Invitrogen), resulting in the creation of in-frame fusion of GFP to the C-terminus of At4g16800. This construct was then introduced into *Agrobacterium tumefaciens* C58C1 using triparental mating. The transformed cells were then co-infiltrated into the abaxial side of the leaves of *N. benthamiana* with an *A. tumefaciens* strain harboring pLN3639 that allowed expression of a N-terminal fragment of isovaleryl-CoA dehydrogenase fused to RFP as a marker of mitochondria (Block *et al.*, 2014). *Nicotiana benthamiana* epidermal cells were imaged by confocal laser-scanning microscopy 48 h later at room temperature using a Nikon 90i microscope equipped with Plan Apo VC60x WI DIC N2 optics, a Nikon A1 camera and acquisition software NIS-Element 4.40.00.

Expression of recombinant At4g16800, protein extractions and enzymatic assays

A truncated version of the At4g16800 protein lacking its predicted N-terminal pre-sequence (residues 1–42) was generated by amplification of *At4g16800* cDNA with primers 5′- CAGTTA*GCTAGC*GT CAAGCTTAATCGTCTATCTG-3′ (forward) and 5′-G*GAATTC*TCAAT TGCCAGTGTACAGAGG-3′ (reverse), which contained the *NheI* and *EcoRI* restriction sites (italicized), respectively. The NheI/EcoRI-digested PCR product was then cloned into the corresponding sites of pET-28a (Novagen, Madison, WI, USA) resulting in an in-frame fusion of a 6xHis tag to the N-terminal end of At4g16800. This construct was introduced in *E. coli* BL21 (DE3) plysS, and protein expression was induced in Luria-Bertani medium containing 0.5 mM isopropyl β-D-1-thiogalactopyranoside for 16 h at 18°C. Cells were harvested by centrifugation and disrupted in phosphate-buffered saline (PBS) buffer (137 mM NaCl, 2.7 mM KCl, 10 mM Na_2HPO_4, 1.8 mM KH_2PO_4 pH 7.5) using sonication. The extract was cleared by centrifugation, and the recombinant protein was purified under native conditions using Ni-NTA agarose. The purified enzyme was desalted on a PD-10 column equilibrated with PBS buffer containing 10% glycerol (vol/vol) and 2 mM dithiothreitol (DTT). The desalted enzyme was frozen in liquid N_2 and stored at −80°C. Arabidopsis rosette leaves (0.1–0.2 g) and seeds (500) were extracted in 2 ml of extraction buffer [150 mM KH_2PO_4 pH 7.5, 10 mM KCl, 2 mM DTT, 3% (w/vol) polyvinylpolypyrrolidone] using a Pyrex tissue grinder. The grinder was washed twice with 1 ml of extraction buffer, and the washes were combined to the initial extract. Samples were then centrifuged (18 000 ***g*** for 5 min at 4°C), and the supernatants (2.5 ml) were desalted on PD-10 columns (GE Healthcare) pre-equilibrated with 150 mM KH_2PO_4, pH 7.5, 10 mM KCl and 2 mM DTT. The desalted extracts were stored as aliquots at −80°C. Assays (100 μl) contained 100 mM Tris-HCl (pH 8.0), 10 mM EDTA, 1 g L^{-1} bovine serum albumin, 0–150 μM HMG-CoA, and 0.125 ng (purified recombinant enzyme) or 1.3–10 μg of protein (desalted Arabidopsis extract). Reactions were performed for 5–20 min at 30°C. The reaction was terminated by adding 10 μl of 2 M HCl. The formation of 3-methylglutaconyl-CoA was quantified by reverse-phase HPLC coupled to spectrophotometric detection, as previously described (Loupatty *et al.*, 2004). Kinetic parameters were calculated using curve fitting with non-linear regression of R studio (https://www.rstudio.com).

Amino acid and ubiquinone analyses

For the quantification of free amino acids, Arabidopsis seeds (300) and rosette leaves (20–90 mg) were spiked with 5 μl (seeds) or 10 μl (leaves) of 2 mM α-aminobutyrate as an internal standard and ground using a glass-rod potter in 300 μl (seeds) or 500 μl (leaves) of 80% (vol/vol) methanol. The potter was then washed with 300 μl (seeds) or 500 μl (leaves) of 80% (vol/vol) methanol, and the wash was combined to the extract. Samples were then cleared twice by centrifugation (18 000 ***g*** for 10 min at 4°C) and supernatants (100 μl) were mixed with 60 μl of water. For the quantification of total amino acids, Arabidopsis seeds (100) and rosette leaves (50–120 mg) were spiked with 5 μl (seeds) or 10 μl (leaves) of 20 mM α-aminobutyrate as an internal standard, and ground using a Pyrex tissue grinder in 300 μl (seeds) or 500 μl (leaves) of extraction buffer containing 20 mM Tris-HCl pH 7.5, 150 mM NaCl. The grinder was then washed with the same volume of extraction buffer and the washes were combined to the initial extracts. Protein hydrolysis was performed by mixing 75 μl of protein extract with 225 μl of 8 N HCl in a 0.3-ml chemical synthesis vial and incubation at 117°C for 24 h. Samples were then evaporated to dryness with gaseous nitrogen at 60°C and resuspended in 1 ml 0.01 N HCl. Hydrolyzed extracts (1 ml) were then loaded on a 15 × 5 mm column packed with Dowex 50wx8 100–200 mesh resin (ACROS Organics) pre-activated with 1 N HCl. The column was washed with 5 ml of water and amino acids were eluted with 5 ml of 1 N NH_4OH. The eluate was evaporated to dryness under gaseous N_2 and resuspended in 500 μl of 50% (vol/vol) methanol. Amino acids were derivatized with *o*-phthalaldehyde prior to separation by reverse-phase HPLC on an Agilent Eclipse XDB-C18 column coupled to fluorometric detection as described in Noctor *et al.* (2007). Amino acids were quantified according to their respective external standards and corrected for recovery. When necessary, samples were diluted with 50% (vol/vol) methanol prior to derivatization, so as for each amino acid level to fit within the ranges of its corresponding standard curve. Quantification of ubiquinone-9 in Arabidopsis rosette leaves and seeds using reverse-phase HPLC separation coupled to diode array detection was performed as previously described (Ducluzeau *et al.*, 2012). Proteins were quantified using the Bradford method with IgG as a standard (Bradford, 1976).

ACKNOWLEDGEMENTS

This work was made possible in part by National Science Foundation Grant MCB-1608088 and MCB-1712608 (to G.J.B.), and IOS-1025636 (to E.P.). The authors thank A.P. Alonso and J.-C. Cocuron (Ohio State University) for their expert advice on the acidic hydrolysis of plant proteins and the subsequent purification of amino acids.

CONFLICT OF INTEREST

The authors declare no conflict of interest.

SUPPORTING INFORMATION

Additional Supporting Information may be found in the online version of this article.

Figure S1. Expression of *At4g16800* in Arabidopsis organs. Data were retrieved from the Arabidopsis eFP Browser (http://www.bar.utoronto.ca/efp/cgi-bin/efpWeb.cgi).

Figure S2. Molecular characterization of *at4g16800* T-DNA insertion mutants.

Figure S3. Levels of free leucine, isoleucine and valine in the rosette leaves of wild-type (Col-0) and T-DNA lines SAIL_428_H01, SALK_072957 and SALK_026612C.

Figure S4. Ubiquinone levels in Arabidopsis leaves and seeds.

Table S1. Predicted subcellular localization of At4g16800

Table S2. Phenotypic analysis of wild-type and *at4g16800* knockout plants

Dataset S1. Correlation ranks and functional annotations mined from the ATTED-II and GeneCAT databases.

Video S1. Time-lapse acquisitions of GFP-tagged At4g16800 transiently expressed in tobacco epidermal cells.

REFERENCES

Alonso, J.M., Stepanova, A.N., Leisse, T.J. *et al.* (2003) Genome-wide insertional mutagenesis of Arabidopsis thaliana. *Science*, **301**, 653–657.

Angelovici, R., Lipka, A.E., Deason, N., Gonzalez-Jorge, S., Lin, H., Cepela, J., Buell, R., Gore, M.A. and Dellapenna, D. (2013) Genome-wide analysis of branched-chain amino acid levels in Arabidopsis seeds. *Plant Cell*, **25**, 4827–4843.

Aoki, Y., Okamura, Y., Tadaka, S., Kinoshita, K. and Obayashi, T. (2016) ATTED-II in 2016: a plant coexpression database towards lineage-specific coexpression. *Plant Cell Physiol.* **57**, e5.

Araújo, W.L., Ishizaki, K., Nunes-Nesi, A. *et al.* (2010) Identification of the 2-hydroxyglutarate and isovaleryl-CoA dehydrogenases as alternative electron donors linking lysine catabolism to the electron transport chain of Arabidopsis mitochondria. *Plant Cell*, **22**, 1549–1563.

Araújo, W.L., Tohge, T., Ishizaki, K., Leaver, C.J. and Fernie, A.R. (2011) Protein degradation – an alternative respiratory substrate for stressed plants. *Trends Plant Sci.* **16**, 489–498.

Bannai, H., Tamada, Y., Maruyama, O., Nakai, K. and Miyano, S. (2002) Extensive feature detection of N-terminal protein sorting signals. *Bioinformatics*, **18**, 298–305.

Binder, S. (2010) Branched-chain amino acid metabolism in Arabidopsis thaliana. *Arabidopsis Book*, **8**, e0137.

Block, A., Widhalm, J.R., Fatihi, A. *et al.* (2014) The origin and biosynthesis of the benzenoid moiety of ubiquinone (Coenzyme Q) in Arabidopsis. *Plant Cell*, **26**, 1938–1948.

Bradford, M.M. (1976) A rapid and sensitive method for the quantification of microgram quantities of protein utilizing the principle of protein-dye binding. *Anal. Biochem.* **72**, 248–254.

Brown, G.K., Hunt, S.M., Scholem, R., Fowler, K., Grimes, A., Mercer, J.F., Truscott, R.M., Cotton, R.G., Rogers, J.G. and Danks, D.M. (1982) Beta-hydroxyisobutyryl coenzyme A deacylase deficiency: a defect in valine metabolism associated with physical malformations. *Pediatrics*, **70**, 532–538.

Buchanan-Wollaston, V., Page, T., Harrison, E. *et al.* (2005) Comparative transcriptome analysis reveals significant differences in gene expression and signalling pathways between developmental and dark/starvation-induced senescence in Arabidopsis. *Plant J.* **42**, 567–585.

Clough, S.J. and Bent, A.F. (1998) Floral dip: a simplified method for Agrobacterium-mediated transformation of Arabidopsis thaliana. *Plant J.* **16**, 735–743.

Di Rosa, G., Deodato, F., Loupatty, F.J. *et al.* (2006) Hypertrophic cardiomyopathy, cataract, developmental delay, lactic acidosis: a novel subtype of 3-methylglutaconic aciduria. *J. Inherit. Metab. Dis.* **29**, 546–550.

Ding, G., Che, P., Ilarslan, H., Wurtele, E.S. and Nikolau, B.J. (2012) Genetic dissection of methylcrotonyl CoA carboxylase indicates a complex role for mitochondrial leucine catabolism during seed development and germination. *Plant J.* **70**, 562–577.

Disch, A., Hemmerlin, A., Bach, T.J. and Rohmer, M. (1998) Mevalonate-derived isopentenyl diphosphate is the biosynthetic precursor of ubiquinone prenyl side chain in tobacco BY-2 cells. *Biochem. J.* **331**, 615–621.

Ducluzeau, A.-L., Wamboldt, Y., Elowsky, C.G., Mackenzie, S.A., Schuurink, R.C. and Basset, G.J. (2012) Gene network reconstruction identifies the authentic trans-prenyl diphosphate synthase that makes the solanesyl moiety of ubiquinone-9 in Arabidopsis. *Plant J.* **69**, 366–375.

Dunshea, F.R., Bauman, D.E., Nugent, E.A., Kerton, D.J., King, R.H. and McCauley, I. (2005) Hyperinsulinaemia, supplemental protein and branched-chain amino acids when combined can increase milk protein yield in lactating sows. *Br. J. Nutr.* **93**, 325–332.

Emanuelsson, O., Nielsen, H., Brunak, S. and von Heijne, G. (2000) Predicting subcellular localization of proteins based on their N-terminal amino acid sequence. *J. Mol. Biol.* **300**, 1005–1016.

Engqvist, M.K., Kuhn, A., Wienstroer, J., Weber, K., Jansen, E.E., Jakobs, C., Weber, A.P. and Maurino, V.G. (2010) Plant D-2-hydroxyglutarate dehydrogenase participates in the catabolism of lysine especially during senescence. *J. Biol. Chem.* **286**, 11382–11390.

Eubel, H., Meyer, E.H., Taylor, N.L., Bussell, J.D., O'Toole, N., Heazlewood, J.L., Castleden, I., Small, I.D., Smith, S.M. and Millar, A.H. (2008) Novel proteins, putative membrane transporters, and an integrated metabolic network are revealed by quantitative proteomic analysis of Arabidopsis cell culture peroxisomes. *Plant Physiol.* **148**, 1809–1829.

Galili, G., Avin-Wittenberg, T., Angelovici, R. and Fernie, A.R. (2014) The role of photosynthesis and amino acid metabolism in the energy status during seed development. *Front. Plant Sci.* **5**, 447.

Galili, G., Amir, R. and Fernie, A.R. (2016) The regulation of essential amino acid synthesis and accumulation in plants. *Annu. Rev. Plant Biol.* **67**, 153–178.

Gerbling, H. and Gerhardt, B. (1989) Peroxisomal degradation of branched-chain 2-oxo acids. *Plant Physiol.* **91**, 1387–1392.

Ginger, M.L., Chance, M.L., Sadler, I.H. and Goad, L.J. (2001) The biosynthetic incorporation of the intact leucine skeleton into sterol by the trypanosomatid Leishmania mexicana. *J. Biol. Chem.* **276**, 11674–11682.

Gipson, A.B., Morton, K.J., Rhee, R.J. *et al.* (2017) Disruptions in valine degradation affect seed development and germination in Arabidopsis. *Plant J.* **90**, 1029–1039.

Gu, L., Jones, A.D. and Last, R.L. (2010) Broad connections in the Arabidopsis seed metabolic network revealed by metabolite profiling of an amino acid catabolism mutant. *Plant J.* **61**, 579–590.

Hildebrandt, T.M., Nunes Nesi, A., Araújo, W.L. and Braun, H.P. (2015) Amino acid catabolism in plants. *Mol. Plant*, **8**, 1563–1579.

Holden, H.M., Benning, M.M., Haller, T. and Gerlt, J.A. (2001) The crotonase superfamily: divergently related enzymes that catalyze different reactions involving acyl coenzyme a thioesters. *Acc. Chem. Res.* **34**, 145–157.

Horton, P., Park, K.J., Obayashi, T., Fujita, N., Harada, H., Adams-Collier, C.J. and Nakai, K. (2007) WoLF PSORT: protein localization predictor. *Nucleic Acids Res.* **35**, W585–W587.

Murakami, T., Kaneko, T., Takeda, S., Inoue, S., Nomoto, S., Koshikawa, K., Nonami, T. and Nakao, A. (2001) Human liver disease decreases methacrylyl-CoA hydratase and beta-hydroxyisobutyryl-CoA hydrolase activities in valine catabolism. *Clin. Chim. Acta*, **312**, 115–121.

Ishizaki, K., Larson, T.R., Schauer, N., Fernie, A.R., Graham, I.A. and Leaver, C.J. (2005) The critical role of Arabidopsis electron-transfer flavoprotein: ubiquinone oxidoreductase during dark-induced starvation. *Plant Cell*, **17**, 2587–2600.

Ishizaki, K., Schauer, N., Larson, T.R., Graham, I.A., Fernie, A.R. and Leaver, C.J. (2006) The mitochondrial electron transfer flavoprotein complex is essential for survival of Arabidopsis in extended darkness. *Plant J.* **47**, 751–760.

Karimi, M., Inze, D. and Depicker, A. (2002) GATEWAY vectors for Agrobacterium-mediated plant transformation. *Trends Plant Sci.* **7**, 193–195.

Kleinboelting, N., Huep, G., Kloetgen, A., Viehoever, P. and Weisshaar, B. (2012) GABI-Kat SimpleSearch: new features of the Arabidopsis thaliana T-DNA mutant database. *Nucleic Acids Res.* **40**, D1211–D1215.

Lange, P.R., Eastmond, P.J., Madagan, K. and Graham, I.A. (2004) An Arabidopsis mutant disrupted in valine catabolism is also compromised in peroxisomal fatty acid beta-oxidation. *FEBS Lett.* **571**, 147–153.

Loupatty, F.J., Ruiter, J.P.N., IJlst, L., Duran, M. and Wanders, R.J.A. (2004) Direct nonisotopic assay of 3-methylglutaconyl-CoA hydratase in

cultured human skin fibroblasts to specifically identify patients with 3-methylglutaconic aciduria type I. *Clin. Chem.* **50**, 1447–1450.

Lu, Y., Savage, L.J., Larson, M.D., Wilkerson, C.G. and Last, R.L. (2011) Chloroplast 2010: a database for large-scale phenotypic screening of Arabidopsis mutants. *Plant Physiol.* **155**, 1589–1600.

Mack, M., Liesert, M., Zschocke, J., Peters, V., Linder, D. and Buckel, W. (2006a) 3-Methylglutaconyl-CoA hydratase from Acinetobacter sp. *Arch. Microbiol.* **185**, 297–306.

Mack, M., Schniegler-Mattox, U., Peters, V., Hoffmann, G.F., Liesert, M., Buckel, W. and Zschocke, J. (2006b) Biochemical characterization of human 3-methylglutaconyl-CoA hydratase and its role in leucine metabolism. *FEBS J.* **273**, 2012–2022.

Millar, A.H., Sweetlove, L.J., Giegé, P. and Leaver, C.J. (2001) Analysis of the Arabidopsis mitochondrial proteome. *Plant Physiol.* **127**, 1711–1727.

Miyashita, Y. and Good, A.G. (2008) NAD(H)-dependent glutamate dehydrogenase is essential for the survival of Arabidopsis thaliana during dark-induced carbon starvation. *J. Exp. Bot.* **59**, 667–680.

Murgas Torrazza, R., Suryawan, A., Gazzaneo, M.C., Orellana, R.A., Frank, J.W., Nguyen, H.V., Fiorotto, M.L., El-Kadi, S. and Davis, T.A. (2010) Leucine supplementation of a low-protein meal increases skeletal muscle and visceral tissue protein synthesis in neonatal pigs by stimulating mTOR-dependent translation initiation. *J. Nutr.* **140**, 2145–2152.

Mutwil, M., Obro, J., Willats, W.G. and Persson, S. (2008) GeneCAT-novel webtools that combine BLAST and co-expression analyses. *Nucleic Acids Res.* **36**, W320–W326.

Noctor, G., Bergot, G., Mauve, C., Thominet, D., Lelarge-Trouverie, C. and Prioul, J.-L. (2007) A comparative study of amino acid measurement in leaf extracts by gas chromatography-time of flight-mass spectrometry and high performance liquid chromatography with fluorescence detection. *Metabolomics*, **3**, 161–174.

Overbeek, R., Begley, T., Butler, R.M. *et al.* (2005) The subsystems approach to genome annotation and its use in the project to annotate 1000 genomes. *Nucleic Acids Res.* **33**, 5691–5702.

Peng, C., Uygun, S., Shiu, S.H. and Last, R.L. (2015) The impact of the branched-chain ketoacid dehydrogenase complex on amino acid homeostasis in Arabidopsis. *Plant Physiol.* **169**, 1807–1820.

Pires, M.V., Júnior, A.A., Medeiros, D.B. *et al.* (2016) The influence of alternative pathways of respiration that utilize branched-chain amino acids following water shortage in Arabidopsis. *Plant Cell Environ.* **39**, 1304–1319.

Pratelli, R. and Pilot, G. (2014) Regulation of amino acid metabolic enzymes and transporters in plants. *J. Exp. Bot.* **65**, 5535–5556.

Reumann, S., Babujee, L., Ma, C., Wienkoop, S., Siemsen, T., Antonicelli, G.E., Rasche, N., Lüder, F., Weckwerth, W. and Jahn, O. (2007) Proteome analysis of Arabidopsis leaf peroxisomes reveals novel targeting peptides, metabolic pathways, and defense mechanisms. *Plant Cell*, **19**, 3170–3193.

Rodríguez, J.M., Ruíz-Sala, P., Ugarte, M. and Peñalva, M.A. (2004) Fungal metabolic model for type I 3-methylglutaconic aciduria. *J. Biol. Chem.* **279**, 32385–32392.

Schertl, P., Danne, L. and Braun, H.-P. (2017) 3-Hydroxyisobutyrate dehydrogenase is involved in both, valine and isoleucine degradation in Arabidopsis thaliana. *Plant Physiol.* **175**, 51–61.

Sessions, A., Burke, E., Presting, G. *et al.* (2002) A high-throughput Arabidopsis reverse genetics system. *Plant Cell*, **14**, 2985–2994.

Shimomura, Y., Murakami, T., Fujitsuka, N., Nakai, N., Sato, Y., Sugiyama, S., Shimomura, N., Irwin, J., Hawes, J.W. and Harris, R.A. (1994) Purification and partial characterization of 3-hydroxyisobutyryl-coenzyme A hydrolase of rat liver. *J. Biol. Chem.* **269**, 14248–14253.

Small, I., Peeters, N., Legeai, F. and Lurin, C. (2004) Predotar: a tool for rapidly screening proteomes for N-terminal targeting sequences. *Proteomics*, **4**, 1581–1590.

Taylor, N.L., Heazlewood, J.L., Day, D.A. and Millar, A.H. (2004) Lipoic acid-dependent oxidative catabolism of alpha-keto acids in mitochondria provides evidence for branched-chain amino acid catabolism in Arabidopsis. *Plant Physiol.* **134**, 838–848.

Vranová, E., Coman, D. and Gruissem, W. (2013) Network analysis of the MVA and MEP pathways for isoprenoid synthesis. *Annu. Rev. Plant Biol.* **64**, 665–700.

Wong, B.J. and Gerlt, J.A. (2004) Evolution of function in the crotonase superfamily: (3S)-methylglutaconyl-CoA hydratase from Pseudomonas putida. *Biochemistry*, **43**, 4646–4654.

Xing, A. and Last, R.L. (2017) A regulatory hierarchy of the Arabidopsis branched-chain amino acid metabolic network. *Plant Cell*, **29**, 1480–1499.

Zhang, S., Chu, L., Qiao, S., Mao, X. and Zeng, X. (2016) Effects of dietary leucine supplementation in low crude protein diets on performance, nitrogen balance, whole-body protein turnover, carcass characteristics and meat quality of finishing pigs. *Anim. Sci. J.* **87**, 911–920.